GEOLOGY | THE GEOLOGICAL SOCIETY OF AMERICA®

https://doi.org/10.1130/G46019.1

Manuscript received 17 January 2019
Revised manuscript received 28 February 2019
Manuscript accepted 28 February 2019

Published online 22 March 2019

A library of early Cambrian chemostratigraphic correlations from a reproducible algorithm

Carling C. Hay[1], Jessica R. Creveling[2], Cedric J. Hagen[2], Adam C. Maloof[3], and Peter Huybers[4]
[1]Department of Earth and Environmental Sciences, Boston College, Chestnut Hill, Massachusetts 02467, USA
[2]College of Earth, Ocean, and Atmospheric Sciences, Oregon State University, Corvallis, Oregon 97330, USA
[3]Department of Geosciences, Princeton University, Princeton, New Jersey 08544, USA
[4]Department of Earth and Planetary Sciences, Harvard University, Cambridge, Massachusetts 02138, USA

ABSTRACT

The visual alignment of chemostratigraphic excursions enables correlation of sedimentary successions within the bounds of geochronology or biostratigraphy. This correlation facilitates the extrapolation of ages from radiometrically calibrated stratigraphic sections to others lacking temporal constraints. For Ediacaran and Cambrian applications, this practice commonly involves assigning ages to fossil first appearances, thereby resolving the tempo of early animal evolution. Chronologies, and the resulting evolutionary insights that they permit, frequently rely on the identification of a single, unique alignment between a time-calibrated and a time-uncertain section, yet visual correlation methods do not permit evaluating the uniqueness of such a chronology. Here we use a dynamic programming algorithm to determine a range of alignments between stratigraphic sections that are optimal under certain assumptions about total temporal overlap and sedimentation rates. We apply the algorithm to radiometrically calibrated Cambrian $\delta^{13}C_{carb}$ records to catalog a library of statistically significant and reproducible alignments. While a subset of the dynamic programming alignments support the statistical significance of published visual alignments, the remaining yield additional, significant correlation solutions that do not violate lithostratigraphic constraints. We conclude that the range of temporal inferences for fossil first appearances that arise from multiple chemostratigraphic alignments should be accounted for in assessing the timing of early Cambrian animal diversification.

INTRODUCTION

Geologists utilize temporal changes in the stable isotopic composition of carbonate rock ($\delta^{13}C_{carb}$) to correlate marine stratigraphic sections around the globe (e.g., Halverson et al., 2005; Saltzman, 2005). For most pre-Quaternary carbonate sections, $\delta^{13}C_{carb}$ correlation relies on visual alignment of excursion peaks and nadirs. Despite large signals, alignments can be hampered by regional heterogeneity arising from local water column processes and syndepositional or diagenetic alteration (Melim et al., 2002). Even when a global signal is preserved, discontinuous sedimentation subsamples an evolving chemical reservoir, thereby truncating or expanding, and amplifying or diminishing, one geochemical sequence relative to another (Cozzi et al., 2004). Finite geochemical sampling and finite resolution of preserved deposits lead to aliasing and smoothing of higher-frequency fluctuations (Myrow and Grotzinger, 2000; Laepple and Huybers, 2013). Finally, quasi-periodic variations in chemostratigraphic records may simultaneously allow for a good fit and a misalignment of cycles. The complexities of the stratigraphic record thus pose a challenge for robust visual alignment of chemostratigraphic records.

But, insomuch as $\delta^{13}C_{carb}$ excursions covary between sites of interest, they facilitate interpolation and extrapolation of radiometric dates and biostratigraphic constraints. One such example is the visual alignment of radiometrically dated $\delta^{13}C_{carb}$ excursions from Cambrian Series 1 (Terreneuvian) and Series 2 shallow marine strata of the Anti-Atlas mountains, Morocco (Maloof et al., 2010b), to undated $\delta^{13}C_{carb}$ sequences sampled at remote, fossiliferous successions to assign ages to the first appearance of animals (Maloof et al., 2010a; Smith et al., 2016; Kouchinsky et al., 2007).

Keeping in mind "that it is difficult to instill geological wisdom into a mathematical process" (Shackleton et al., 1995, p. 694), we seek to evaluate the reproducibility and uniqueness of visual correlation of Cambrian $\delta^{13}C_{carb}$ records. We apply a computationally efficient numerical methodology based on dynamic programming to align chemostratigraphic data. Alignments maximize correlation, subject to constraints upon inserting hiatuses into either record, and the degree to which records must overlap (Sakoe and Chiba, 1978; Clark, 1985; Lisiecki and Lisiecki, 2002). Dynamic programming has been used to align Quaternary $\delta^{18}O_{carb}$ records (Lisiecki and Lisiecki, 2002; Haam and Huybers, 2010). Analogous sequencing algorithms, such as graphical correlation and immutable slotting, underpin the well-resolved Ordovician and Silurian time scales (Sadler, 2004; Sadler and Cooper, 2008). To our knowledge, this contribution is the first application of the technique for the purpose of cataloguing a library of possible chemostratigraphic alignments.

METHODOLOGY

We explore an intrabasinal application of numerical $\delta^{13}C_{carb}$ alignment such that lithostratigraphy serves as an independent guide to correlation. We adopt an ~2-km-thick, stratigraphically continuous and radiometrically calibrated Cambrian Series 1–2 $\delta^{13}C_{carb}$ curve (section 16, or S16, from Sidi M'Sal, Anti-Atlas, Morocco; Maloof et al., 2010b) as the "target" sequence and employ dynamic programming to explore the suite of alignments to two time-uncertain candidate $\delta^{13}C_{carb}$ sequences that lithostratigraphy suggests should overlap a subset of S16. The first, section 3 (S3) at Talat N' Yissi, is located ~35 km south of S16, and the second, section 11 (S11) at North Zawyat n' Bougzoul, is ~200 km northeast of S16 (Maloof et al., 2005).

Dynamic programming involves constructing an n by m cost matrix (C) of all possible matches between data from two sequences. Each element of the matrix is computed as the squared difference between a data point in the target sequence (x_n) and the candidate sequence (y_m): $C(n,m) = (x_n - y_m)^2$.

CITATION: Hay, C.C., et al., 2019, A library of early Cambrian chemostratigraphic correlations from a reproducible algorithm: Geology, v. 47, p. 457–460, https://doi.org/10.1130/G46019.1

Alignment takes the form of a warping path p that assigns each index, m, from the candidate sequence to an index, n, of the target sequence, $n = p(m)$. An optimal path can be efficiently found using linear programming to minimize the sum of the cost matrix across all m (Sakoe and Chiba, 1978). An alignment path that preserves the original sequence would give $n = m$, whereas inserting a depositional hiatus in the target sequence (stretching) takes the form of $p(m + 1) > p(m) + 1$, and inserting a hiatus in the candidate sequence (squeezing) corresponds to $p(m + 1) = p(m)$ (Fig. DR1 in the GSA Data Repository[1]).

Alignment of the candidate and target sequences by stretching and squeezing depends on two stratigraphically meaningful parameters. The edge parameter (Sakoe and Chiba, 1978) relates to whether the two sections span the same interval of time, and penalizes those points in the candidate sequence that lie outside the time span of the target sequence. Large edge values ($>10^3$) force 100% overlap between the sequences, whereas other formulations allow the top and base of the candidate sequence to extend beyond the time represented by the target sequence. To focus attention on physically plausible intrabasinal correlations, we only consider alignments with >10% overlap. The g parameter (Sakoe and Chiba, 1978) relates to the similarity of sediment accumulation rates at the two stratigraphic sections during their shared interval of deposition and tabulates the penalty for inserting hiatuses into the target and/or the candidate sequence. Values of $g > 1$ penalize stretching or squeezing, whereas the converse is the case for values <1. For alignments with <100% overlap, we scale the chronology of the non-overlapping candidate data by the average factor of stretching or squeezing from the overlapping portion of the sequences. Alignments are determined using a dynamic programming method (Sakoe and Chiba, 1978; Clark, 1985; Lisiecki and Lisiecki, 2002; Lisiecki and Raymo, 2005). The code is provided in the Data Repository.

For this application, we assume a global signal and retain the primary magnitude of isotopic excursions in the two sequences to leverage greater information from each record by using both the mean values and the isotopic variability as constraints on alignment. Alternatively, normalizing excursions to have the same mean and variance facilitates alignment of geochemical data across isotopic gradients or of different units (e.g., per mil versus parts per million).

We report the statistical significance of alignments by evaluating the null hypothesis of no true correlation using a Monte Carlo method with 10,000 synthetic $\delta^{13}C$ sequences. A sample size of 10,000 synthetics ensures robust statistics with minimal additional computational expense. We realize synthetics using Cholesky's decomposition method and constrain each synthetic sequence to have the same length and autocorrelation as the candidate sequence (Haam and Huybers, 2010). Synthetics are aligned to the target sequence by dynamic programming with a fixed edge parameter (0.2) and g values that span the range produced by the library of solutions for the alignment of the original candidate. The fixed edge value prevents the degenerate case of achieving a high correlation by offsetting the records to share only a small number of data points. To assess statistical significance, we evaluate the average correlation coefficient obtained across all edge values (for each fixed g value) against the distribution of correlation coefficients associated with synthetic alignments.

[1]GSA Data Repository item 2019175, dynamic programming Matlab code; sample cost matrix, alignment path, and alignments; calculations of relative rates of sediment accumulation; and the correlation coefficients and p-values of alignments, is available online at http://www.geosociety.org/datarepository/2019/, or on request from editing@geosociety.org.

REPRODUCING A CAMBRIAN COMPOSITE $\delta^{13}C_{carb}$ CURVE

Aligning Section 3

Alignments between S3 and S16 $\delta^{13}C_{carb}$ sequences are computed for all pairs of edge values from 0.1 to 0.15 at increments of 0.0005 and g values from 0.98 to 1.01 at spacings of 0.005 (Fig. 1A). This approach yields four distinct and significant alignment groupings with >10% overlap relative to a null hypothesis of no correlation (Fig. 1B, alignments $a_{3.1}$–$a_{3.4}$). Table 1 highlights the differences in the mean correlation coefficients and their respective significance levels (p-values). For g values of 0.99 and 0.995, the average correlation coefficients have p-values of 0.05 and 0.01, respectively. Although in both cases the null hypothesis of no relationship can be rejected, it is more difficult to establish that one solution is significantly better than the other. As the goodness of fit between sequences is insufficient for ascertaining correct alignment, we next consider geologic and biostratigraphic constraints in the context of the four objectively determined alignments.

We begin by evaluating $a_{3.1}$ because it appears to be the most easily rejected. This alignment family represents <1% of the total alignments. The edge values associated with this alignment (>0.7) condition the solution to contain S3 within S16 by pairing multiple S3 $\delta^{13}C_{carb}$ values with individual S16 values (Fig. 1B). This alignment implies missing time in S16 from depositional hiatuses or erosion. Although S3 contains no skeletal fossils, the upper half of the section has a lithostratigraphic affinity to the Igoudine, Amouslek, and Issafene Formations (Fig. 1C) that elsewhere host Cambrian Series 2 trilobites and archaeocyaths (Geyer and Landing, 2006). On this basis, Maloof et al. (2010a) aligned the base of S3 to S16 at ~1190 m, above non-fossiliferous strata assigned to Cambrian Series 1 (Fig. 1C). Thus, $a_{3.1}$ correlates trilobite biozones inferred to apply to S3 to pre-trilobitic strata of S16, therefore appearing implausible.

The remaining solutions, $a_{3.2}$–$a_{3.4}$, align S3 $\delta^{13}C_{carb}$ values to the 8‰ excursion from S16 at ~1460–1570 m and variably stretch or squeeze S3 above and below this excursion (Figs. 1B and 1C). Solution $a_{3.3}$ closely reproduces the correlation proposed by Maloof et al. (2010a). Solution $a_{3.4}$ differs only slightly from $a_{3.3}$, and a lower-resolution search of the parameter space could readily miss this small solution space. Solution $a_{3.2}$ (g <1) initiates alignment lower in S16 than solution $a_{3.3}$ and implies more continuous deposition at S16 than at S3.

Alignments $a_{3.2}$–$a_{3.4}$ variably correlate strata assigned to the Lie de Vin and Igoudine Formations at S3 to the same formations at S16, thereby providing a measure of the diachroneity of lithostratigraphic units between sections. Alignment $a_{3.3}$ invokes the least diachroneity by correlating the base of the Lie de Vin Formation thrombolitic carbonate at S3 to a similarly generalized lithologic package at S16 (Fig. 1C, base of long-dashed lines). Alignment $a_{3.2}$ invokes the greatest diachroneity, requiring that the base of the Lie de Vin Formation at S3 correlate with the top of the Adoudounian Formation at S16 (Fig. 1C, base of dotted lines). Similar to the correlation of Maloof et al. (2010a), $a_{3.2}$–$a_{3.4}$ imply that strata assigned to the Igoudine Formation at S3 are wholly younger than strata assigned to the same formation at S16 (Fig. 1C).

Following Maloof et al. (2010a), we calculate three linear sedimentation rates between the four radiometric dates at S16 to develop an age model for all strata (meterage) between these horizons. For S16 strata cropping out above or below the radiometric dates, we assign ages based on the closest computed sedimentation rate. We then use the dynamic programming $\delta^{13}C_{carb}$ alignment solutions (Fig. 1) to assign these ages to the corresponding S3 meterage and computed the resulting sedimentation rates implied by the three alignments ($a_{3.2}$–$a_{3.4}$). The sediment accumulation rates implied by the alignments differ by more than an order of magnitude. Alignments $a_{3.2}$ and $a_{3.3}$ produce sedimentation rates from 0.5 to 54 cm/k.y. (Fig. 2), while the wider range in sedimentation rates implied by $a_{3.4}$ results from squeezing the lowermost 288 m of S3 into the 76 m below the 520.93 Ma ash bed in S16 (yielding an average rate of 144 cm/k.y.; Fig. 2). This high average sedimentation rate may exclude $a_{3.4}$ as a plausible solution. With a viable age model, one also can provide a quantitative measure of the diachroneity of lithostratigraphic contacts between the target and candidate sections. For instance, a linearly interpolated age model assigns the Lie de Vin–Igoudine Formation contact at S16 an age of 520.46 Ma, whereas all three viable alignment solutions imply an older age for the same contact at S3 (521.03–521.01 Ma). While the absolute value of this diachroneity would change with an alternative age model (e.g., if linear interpolation were inaccurate), the alignment

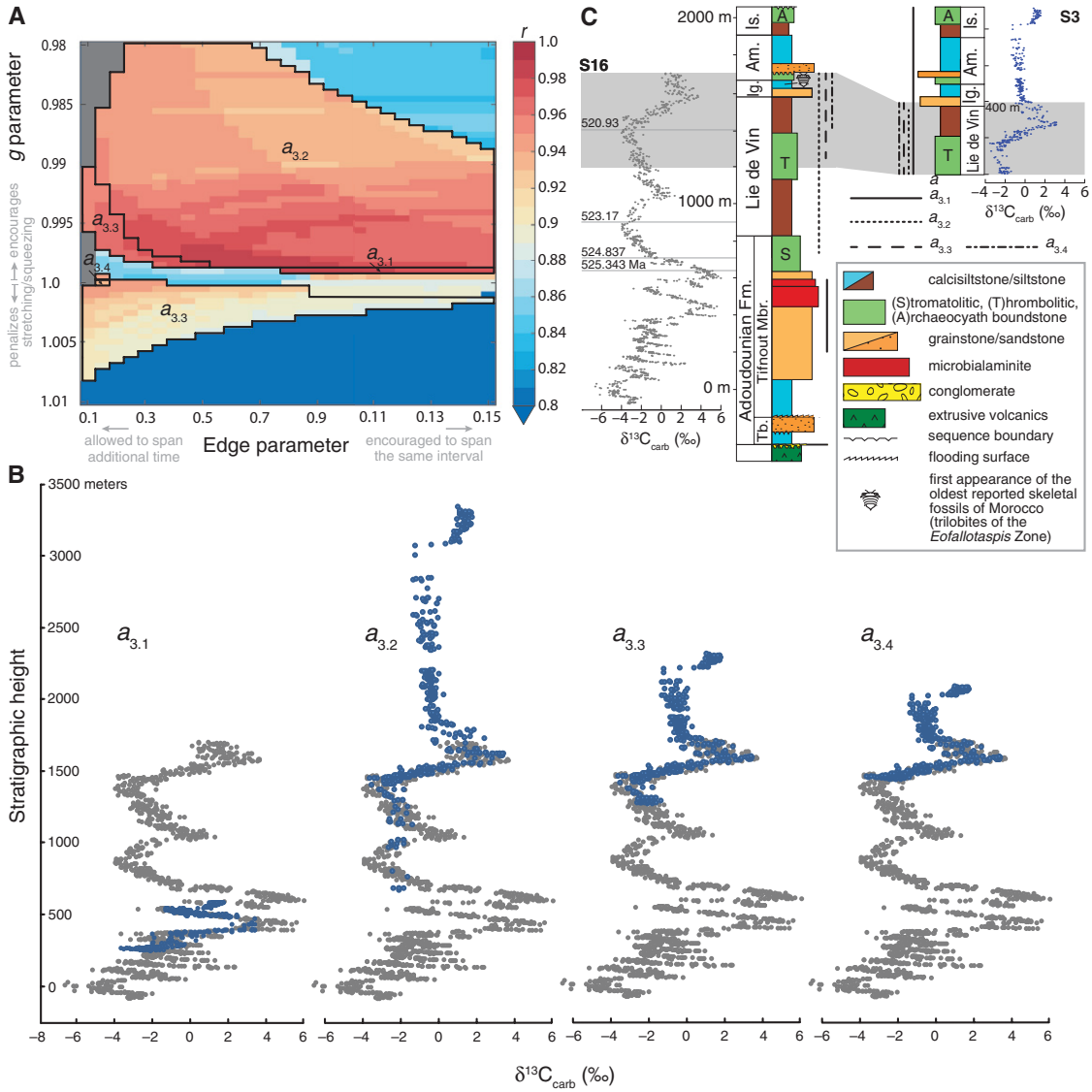

Figure 1. Optimal alignments of Cambrian Series 1–2 $\delta^{13}C_{carb}$ (carb—carbonate) data from sections S3 (Talat N'Yissi) and S16 (Sidi M'Sal), Anti-Atlas, Morocco (Maloof et al., 2005, 2010b). A: Correlation coefficients ($0.8 < r < 1$) for solutions with specified pairings of *g* parameter (relating to the similarity of sediment accumulation rate at two stratigraphic sections during their shared interval of deposition) and edge parameter (relating to whether two sections span the same interval of time) (Sakoe and Chiba, 1978). Gray areas show parameter pairings that yield invalid alignments (<10% overlap). Solid black lines circumscribe parameter space for four distinct and significant alignment solutions ($a_{3.1}$–$a_{3.4}$). B: Alignments $a_{3.1}$–$a_{3.4}$, between S3 $\delta^{13}C$ data (blue) and S16 $\delta^{13}C$ data (gray), that correspond to parameter space in A. C: Lithostratigraphic correlation implied by alignments $a_{3.1}$–$a_{3.4}$. For example, solution $a_{3.1}$ (solid line) correlates $\delta^{13}C_{carb}$ data sampled from all S3 lithostratigraphic units to Adoudounian Formation at S16 (246–580 m). Shading covers visual correlation of Maloof et al. (2010a). Four radiometric dates shown on the S16 chronology are taken from Maloof et al. (2010b). Fm.—Formation; Mbr.—Member; Tb.—Tabia Member; Ig.—Igoudine Formation; Am.—Amouslek Formation; Is.—Issafene Formation.

solutions provide a testable prediction for stratal relationships.

We conclude that $a_{3.3}$, with correlation coefficients >0.9 and reasonable sedimentation rates, reproduces the correlation proposed by Maloof et al. (2010a), and that $a_{3.2}$ and $a_{3.4}$ provide plausible and previously unconsidered alternatives that accord with published litho- and biostratigraphic constraints (Fig. 1C). The conclusion of multiple valid chemostratigraphic correlation solutions bears on the temporal framework for early Cambrian fossil first appearances. If a hypothetical fossil first appeared in the basal stratum of S3, then the three plausible alignment solutions to S16 imply a range of first appearance ages from 525.03 Ma ($a_{3.2}$) to 521.25 Ma ($a_{3.4}$) (Fig. 2). This ~4 m.y. uncertainty, arising solely from multiple valid chemostratigraphic alignment solutions, should propagate into assessments of the tempo of Cambrian evolutionary radiation, particularly those arising from interbasinal correlations (Maloof et al., 2010a; Smith et al., 2016). In contrast, if a hypothetical fossil were recovered from the S3 ~8‰ excursion nadir, then the three plausible alignment solutions imply a narrow first appearance datum between 521.15 Ma ($a_{3.2}$) and 521.14 Ma ($a_{3.3}$ and $a_{3.4}$); this precision reflects the confidence of aligning a distinctive $\delta^{13}C_{carb}$ excursion between candidate and target sections, and has implications for the tempo of Cambrian evolution.

Although we provide a large library of possible stratigraphic alignments, these are not exhaustive, nor necessarily representative of all plausible solutions. Furthermore, we cannot exclude that the best parameter selection changes along a chemostratigraphic section, nor that applying other constraints on the solution would generally be more appropriate.

Aligning Section 11

Dynamic programming yields three plausible alignments that correlate Adoudounian Formation strata at S11 and S16 (Fig. 2, $a_{11.3}$–$a_{11.5}$), and other

TABLE 1. AVERAGE CORRELATION COEFFICIENTS AND ASSOCIATED *p*-VALUES FOR THE ALIGNMENT OF SECTION S3 TO SECTION S16 OF CAMBRIAN SERIES 1–2 SHALLOW MARINE STRATA OF THE ANTI-ATLAS MOUNTAINS, MOROCCO, FOR AN EDGE VALUE OF 0.2 AND *g* VALUES FROM 0.99–1.005

Alignment	Edge value	*g* value	Average correlation	*p*-value
S3 to S16	0.2	0.990	0.9399	0.049
	0.2	0.995	0.9680	0.013
	0.2	1.000	0.8857	0.250
	0.2	1.005	0.5384	0.290

Note: Section S3 is from Maloof et al. (2005), Section S16 is from (Maloof et al., 2010b); edge value relates to whether two sections span the same interval of time, *g* value relates to the similarity of sediment accumulation rate at two stratigraphic sections during their shared interval of deposition.

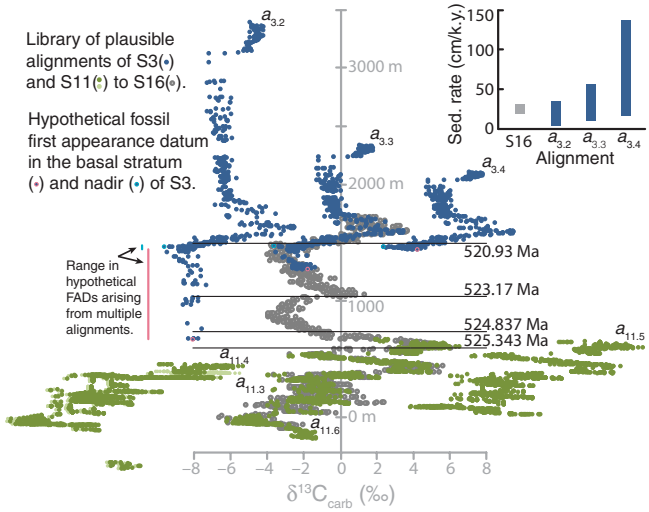

Figure 2. Dynamic programming–derived library of stratigraphically plausible, Cambrian Series 1–2 $\delta^{13}C_{carb}$ (carb—carbonate) alignment solutions for sections S3 (Talat N' Yissi; blue circles; Maloof et al., 2005) and S11 (North Zawyat n' Bougzoul; green circles; Maloof et al., 2005) to section S16 (Sidi M'Sal; gray circles; Maloof et al., 2010b), Anti-Atlas, Morocco. Four radiometric dates shown on the S16 chronology are taken from Maloof et al. (2010b). Inset shows the range of sedimentation rates implied by alignment solutions $a_{3.2}$, $a_{3.3}$, and $a_{3.4}$ (Fig. DR4 [see footnote 1]) compared to that for S16 (Maloof et al., 2010b). Alignment of S11 to S16 strata below the oldest radiometric constraint precludes the calculation of absolute sedimentation rates.

less-favorable solutions (Fig. DR2). Solutions $a_{11.3}$ and $a_{11.4}$ differ in the predicted duration of deposition at S11, with $a_{11.4}$ stretching S11 to encompass an additional high-amplitude excursion (Fig. 2). Unlike $a_{11.3}$–$a_{11.4}$, $a_{11.5}$ reproduces the compelling visual alignment of S11 to S16 between 386 m and 661.5 m in S16 (Maloof et al., 2010a), although this fit begins higher up in S16 (Fig. 2). If robust, then $a_{11.3}$–$a_{11.5}$ imply that S11 deposited more rapidly than previously considered. While solutions $a_{11.3}$ and $a_{11.4}$ hang S11 $\delta^{13}C_{carb}$ values below S16 to produce a composite curve similar to that of Maloof et al. (2010a), this result was not guaranteed. In an alternative analysis, we aligned S11 to S16 after truncating S11 $\delta^{13}C_{carb}$ values from the Tabia Member of the Adoudounian Formation below an unconformity of unknown duration (Fig. 1C); this option yielded one additional solution ($a_{11.6}$) that reproduces the visual alignment of Maloof et al. (2010a). The four major categories of viable alignments between S11 and S16 are depicted in Figure 2.

CHRONOLOGIC IMPLICATIONS AND EVOLUTIONARY CONCLUSIONS

Ideally, a single chemostratigraphic alignment could be determined, though in practice, multiple statistically significant and plausible alignments exist, and all should be catalogued and presented. For the case of aligning S3 to S16, we found four significant solutions, of which one reproduces the previously published visual alignment (Maloof et al., 2010a) and two represent additional solutions that accord with published litho- and biostratigraphic constraints. Aligning S11 to S16 reveals four significant solution sets, of which three represent previously unconsidered alignments that conform to lithostratigraphic constraints and one reproduces the alignment of Maloof et al. (2010a). Dynamic programming–based $\delta^{13}C_{carb}$ alignments between time-calibrated and time-uncertain Cambrian fossil-bearing carbonate sections will yield a library of alignments and, therefore, a *range* of valid first appearance ages that will require a revised conception of the chronology of animal evolution.

ACKNOWLEDGMENTS

Hay, Huybers, Creveling, and Maloof acknowledge support from their universities. Hagen thanks the ARCS Foundation and the National Science Foundation (NSF) Graduate Research Fellowship Program, and Maloof acknowledges NSF grant EAR-1410317. We thank Peter Sadler, editor James Schmitt, and three anonymous reviewers, whose comments greatly improved the manuscript.

REFERENCES CITED

Clark, R.M., 1985, A FORTRAN program for constrained sequence-slotting based on minimum combined path length: Computers & Geosciences, v. 11, p. 605–617, https://doi.org/10.1016/0098-3004(85)90089-5.

Cozzi, A., Allen, P.A., and Grotzinger, J.P., 2004, Understanding carbonate ramp dynamics using $\delta^{13}C$ profiles: Examples from the Neoproterozoic Buah Formation of Oman: Terra Nova, v. 16, p. 62–67, https://doi.org/10.1111/j.1365-3121.2004.00528.x.

Geyer, G., and Landing, E., 2006, Morocco 2006: Ediacaran–Cambrian Depositional Environments and Stratigraphy of the Western Atlas Regions: Explanatory Description and Field Excursion Guide: Beringeria, Special Issue 6, 120 p.

Haam, E., and Huybers, P., 2010, A test for the presence of covariance between time-uncertain series of data with application to the Dongge Cave speleothem and atmospheric radiocarbon records: Paleoceanography, v. 25, PA2209, https://doi.org/10.1029/2008PA001713.

Halverson, G.P., Hoffman, P.F., Schrag, D.P., Maloof, A.C., and Rice, A.H.N., 2005, Toward a Neoproterozoic composite carbon-isotope record: Geological Society of America Bulletin, v. 117, p. 1181–1207, https://doi.org/10.1130/B25630.1.

Kouchinsky, A., Bengtson, S., Pavlov, V., Runnegar, B., Torssander, P., Young, E., and Ziegler, K., 2007, Carbon isotope stratigraphy of the Precambrian–Cambrian Sukharikha River section, northwestern Siberian platform: Geological Magazine, v. 144, p. 609–618, https://doi.org/10.1017/S0016756807003354.

Laepple, T., and Huybers, P., 2013, Reconciling discrepancies between Uk37 and Mg/Ca reconstructions of Holocene marine temperature variability: Earth and Planetary Science Letters, v. 375, p. 418–429, https://doi.org/10.1016/j.epsl.2013.06.006.

Lisiecki, L.E., and Lisiecki, P.A., 2002, Application of dynamic programming to the correlation of paleoclimate records: Paleoceanography, v. 17, 1049, https://doi.org/10.1029/2001PA000733.

Lisiecki, L.E., and Raymo, M.E., 2005, A Pliocene-Pleistocene stack of 57 globally distributed benthic $\delta^{18}O$ records: Paleoceanography, v. 20, PA1003, https://doi.org/10.1029/2004PA001071.

Maloof, A.C., Schrag, D.P., Crowley, J.L., and Bowring, S.A., 2005, An expanded record of Early Cambrian carbon cycling from the Anti-Atlas Margin, Morocco: Canadian Journal of Earth Sciences, v. 42, p. 2195–2216, https://doi.org/10.1139/e05-062.

Maloof, A.C., Porter, S.M., Moore, J.L., Dudas, F.O., Bowring, S.A., Higgins, J.A., Fike, D.A., and Eddy, M.P., 2010a, The earliest Cambrian record of animals and ocean geochemical change: Geological Society of America Bulletin, v. 122, p. 1731–1774, https://doi.org/10.1130/B30346.1.

Maloof, A.C., Ramezani, J., Bowring, S.A., Fike, D.A., Porter, S.M., and Mazouad, M., 2010b, Constraints on early Cambrian carbon cycling from the duration of the Nemakit-Daldynian–Tommotian boundary ^{13}C shift, Morocco: Geology, v. 38, p. 623–626, https://doi.org/10.1130/G30726.1.

Melim, L.A., Westphal, H., Swart, P.K., Eberli, G.P., and Munnecke, A., 2002, Questioning carbonate diagenetic paradigms: Evidence from the Neogene of the Bahamas: Marine Geology, v. 185, p. 27–53, https://doi.org/10.1016/S0025-3227(01)00289-4.

Myrow, P.M., and Grotzinger, J.P., 2000, Chemostratigraphic proxy records: Forward modeling the effects of unconformities, variable sediment accumulation rates, and sampling-interval bias, *in* Grotzinger, J.P., and James, N.P., eds., Carbonate Sedimentation and Diagenesis in the Evolving Precambrian World: SEPM (Society for Sedimentary Geology) Special Publication 67, p. 43–58.

Sadler, P.M., 2004, Quantitative biostratigraphy—Achieving finer resolution in global correlation: Annual Review of Earth and Planetary Sciences, v. 32, p. 187–213, https://doi.org/10.1146/annurev.earth.32.101802.120428.

Sadler, P.M., and Cooper, R.A., 2008, Improved resolution and quantified uncertainty—Time scales of the future: Newsletters on Stratigraphy, v. 43, p. 49–53, https://doi.org/10.1127/0078-0421/2008/0043-0049.

Sakoe, H., and Chiba, S., 1978, Dynamic programming algorithm optimization for spoken word recognition: IEEE Transactions on Acoustics, Speech, and Signal Processing, v. 26, p. 43–49, https://doi.org/10.1109/TASSP.1978.1163055.

Saltzman, M.R., 2005, Phosphorus, nitrogen, and the redox evolution of the Paleozoic oceans: Geology, v. 33, p. 573–576, https://doi.org/10.1130/G21535.1.

Shackleton, N.J., Hagelberg, T.K., and Crowhurst, S.J., 1995, Evaluating the success of astronomical tuning: Pitfalls of using coherence as a criterion for assessing pre-Pleistocene timescales: Paleoceanography, v. 10, p. 693–697, https://doi.org/10.1029/95PA01454.

Smith, E.F., Macdonald, F.A., Petach, T.A., Bold, U., and Schrag, D.P., 2016, Integrated stratigraphic, geochemical, and paleontological late Ediacaran to early Cambrian records from southwestern Mongolia: Geological Society of America Bulletin, v. 128, p. 442–468, https://doi.org/10.1130/B31248.1.

Printed in USA